designs

MDPI

Article

Biomechanical Device for Measurement of Adductors Strength and Aid in Self-Catheterisation of Spastic Patients

Maria Cruz [1,2], Vítor Maranha [1,2,3], Fernando Moita [1,2], Nuno Cruz [1], Deolinda Rasteiro [1,2], Filipe Carvalho [2,4], Jorge Lains [2,4,5] and Luis Roseiro [1,2,3,*]

1 Polytechnic of Coimbra, ISEC, Rua Pedro Nunes—Quinta da Nora, 3030-199 Coimbra, Portugal; ines.p.cruz.98@gmail.com (M.C.); vitor.maranha@isec.pt (V.M.); moita@isec.pt (F.M.); nuno.cruz@isec.pt (N.C.); dml@isec.pt (D.R.)
2 Applied Biomechanics Laboratory, i2A—Institute of Applied Research, Polytechnic of Coimbra, Lagar dos Cortiços–S. Martinho do Bispo, 3030-093 Coimbra, Portugal; filipe.dvcarvalho@yahoo.com (F.C.); jorgelains@sapo.pt (J.L.)
3 Department of Mechanical Engineering, Materials and Processes (CEMMPRE), University of Coimbra, 3030-788 Coimbra, Portugal
4 Centro de Medicina de Reabilitação da Região Centro, Hospital Rovisco Pais, Quinta da Fonte Quente, 3064-908 Tocha, Portugal
5 Faculty of Medicine, University of Coimbra, 3004-504 Coimbra, Portugal
* Correspondence: lroseiro@isec.pt; Tel.: +351-967-845-829

Abstract: Intermittent vesical self-catheterisation is a legitimate and safe technique that has been reported since the 1970s as a solution for the treatment and prevention of vesical urinary complications resulting from spinal cord injury. This practice, using clean technology, has been asserting itself as one of the best alternatives for people with neurogenic bladder. However, adherence is not complete due to some barriers imposed to this procedure by the injured, with emphasis on positioning, agility, and visual impairment. The solutions presented today to support self-catheterisation are expensive equipment that does not allow patients with advanced levels of spasticity to have their autonomy. A biomechanical support device was developed to aid self-catheterisation, mainly aimed at women with spasticity, filling the gap in the existing products. Despite the main objective of self-catheterisation, the system's design made it possible to quantify the strength of the adductors for the sitting position during the execution of the adduction movement, particularly relevant for spastic patients. The device's production was entirely carried out using the FDM methodology, with 3D printers, and its design and operation were thought to overcome the physical and psychological barriers imposed by the users. The system was first tested with a group of healthy volunteers to obtain a pattern of the adductors force in a sitting position and after with a group of spastic volunteers. The obtained data allows to compare the adductor force data and optimize the system, with particular functionalities for spastic patients, with the implementation of a motorised version and a visualization camera. The system, its developments, and results obtained are present and discussed.

Keywords: self-catheterisation; spasticity; adductors strength; biomechanical rehabilitation

Citation: Cruz, M.; Maranha, V.; Moita, F.; Cruz, N.; Rasteiro, D.; Carvalho, F.; Lains, J.; Roseiro, L. Biomechanical Device for Measurement of Adductors Strength and Aid in Self-Catheterisation of Spastic Patients. *Designs* **2022**, *6*, 7. https://doi.org/10.3390/designs6010007

Academic Editor: Richard Drevet

Received: 23 November 2021
Accepted: 17 January 2022
Published: 20 January 2022

1. Introduction

Spinal cord injury is a syndrome that makes a person impaired in motor, sensory, visceral, sexual, and autonomic functions (Assis and Faro, 2011) [1]. There are several possible consequences for this type of injury, such as paralysis, vesico-urinary dysfunction, and spasticity. This work focuses on vesico-urinary dysfunction, termed the product of the interruption of communication between the bladder and the urinary centre in the brain. In the human body, there is, in addition to others, the autonomic nervous system (ANS) and which contains the pelvic splanchnic nerves, which communicate with the brain concerning the urinary bladder and external genital organs. According to

Shenot (2018) [2], the possible treatments for this type of disease include catheterisation or measures to trigger urination. One of the main measures to trigger urination is intermittent urethral catheterisation, designed as self-catheterisation if performed by the patient. This method allows the patient to empty the bladder by introducing a catheter. This process is recommended temporarily or permanently at any age and gender (Mazzo et al., 2014) [3]. Seth et al (2014) [4] report that this type of process has improved quality of life for patients, offering them greater freedom to participate in daily and social activities. However, there is resistance to vesical catheterisation due to practical barriers such as dexterity, positioning, visual impairment, and external factors such as appropriate catheters and assistive devices. Baczkoski [5], in 1981, wrote that there is a considerable number of patients dependent on catheterisation who are independent and can perform self-catheterisation. However, there are still individuals, especially women, who cannot perform it. The most salient reasons are the difficulty visualizing the urogenital triangle area due to its body physiognomy (wrinkled skin, protruding abdomen, large breasts, among other conditions) or its physical condition (inability to flex the spine or weakness in certain positions). Few support devices have been developed and built to overcome these difficulties. For example, in 1968, Levy [6] invented a set formed by a mirror mounted between a pair of clamps, which is placed between the legs, and the individual moving of the legs in various directions can adjust it. The device's purpose was to free an individual's hand, to allow for depilation and the application of make-up. However, for an individual with spasticity, the set is not suitable as the position of the mirror is affected whenever the legs move. In addition, the mechanism for supporting the setup was designed so that the opening of the person's legs is minimal, and any movement with higher amplitude promotes the set to fall. Baczkoski (1981) [5] published a device with a mirror designed to free both patient's hands when the patient needs to carry out personal hygiene and allows viewing parts of the body that are difficult to access under these circumstances. This device will enable patients some autonomy regarding their cleaning, dressing, and catheterisation. This set consists of a mirror that is fixed by mounting elements of an adjustable plate, which has the option of being attached to the lower part of the patient's leg. The recommended position to facilitate the application is lying down, making the process cleaner and safer, but it does not favour the issue of visibility. In 1990, Billau and Howland [7] created three devices that complement each other: a lip expander, female quadriplegic forceps, and an illuminated catheterisation mirror. These solutions are intended for patients with agility and strength in the lower limbs and at least in one of the upper limbs. Following these developments, Gerace (1994) [8] proposed a set adapted for use in self-catheterisation procedures, consisting of a base with a mounted mirror and a pair of claws that are placed on the legs. This set is designed to be mounted on the patient's legs, in a seated position, with the mirror in the centre and between the legs so that she can adjust the base through the opening or closing movement of the legs. The mirror is adjustable for different clinics, and the extension of the leg claws does not change its inclination. The user can also attach a removable mirror to an elongated member with a snap-on flexible fitting. Alvi et al. [9] proposed a mirror with a support member attached to one end of the toilet. There is a hinge on the mirror support member that helps adjust the member for self-inspection.

Advancements with the developed devices offer some help to patients with needs concerning the catheterisation process. However, there is still a need for a complete device, mainly to cover the barriers associated with a self-catheterisation process, for example, spastic patients or patients with weak limb strength. This paper presents a biomechanical device that allows the implementation of the self-catheterisation process by these types of patients.

The literature shows several instruments measuring muscle strength, from dynamometers to weight machines, including traction devices such as the Pivot Fitness 820 [10], or specific tests such as BEP IIIa [11]. Within the dynamometers, there are portable ones such as Smart Groin [12], and isokinetic ones such as Cybex II [13], Power Track 11, Commande [14], KForce Muscle Controller [15], and ForceFrame [16]. All these instruments aim

to measure strength in any individual. However, there are specific instruments for individuals with pathologies, particularly patients with spasticity. Cabrera et al., 2007, [17] proposed a device that, when the extremity is moved around an axis, it is possible to quantify the acceleration, angular velocity, force, and time required for the movement. Subsequently, the acquired values generated the hypertonic condition of the limb. In addition, Wang et al. (2016) [18] presented a device that quantifies spasticity by measuring the speed and strength in the movement of a limb.

Over time, studies were carried out to quantify muscle strength [10,11,13,14,19,20]. They contained the limitation that the strength studied was the abductors. The studied population did not refer to individuals who suffered from spinal cord injury but who had undergone arthroplasty. In 2017, Gafner et al. [21] studied the strength of hip adductors and abductors in the elderly. However, Pinto (2020) [12] carried out a study to evaluate hip strength in elite players in Portugal, and Ryan, Kempton, Pacecca, and Coutts (2019) [22] in professional Australian footballers, assessing the strength of the adductor muscles. The methodology for evaluating of adductors was for the volunteer to exert a contraction against the evaluator. There are several studies like this one that focuses on athletes from different sports. In 2018, a study was carried out by Vega et al. [23], which consisted of evaluating the validity and reliability of the test–retest, through the quantification of the isometric strength of the abductor's muscles, in a healthy young population.

The studies found in the literature differ from this work, mainly due to the group of muscles and movements evaluated (abductor muscles and abduction movement) as well as its sample as it includes elite players from different sports or people recovering from surgery, leaving space for the study of ordinary healthy citizens and people with spinal injury and spasticity.

The presented device, like some others, has a load cell attached. However, it differs from other devices, providing the possibility to adjust the opening of the thighs, allowing the measurement for different degrees of space and the evaluation of the two thighs simultaneously. The device developed allowed us to perform a study to obtain and compare healthy young individuals with people with spinal cord injury.

2. Materials and Methods

2.1. Device Development—3D Models

The 3D geometry of the models was created using Solidworks® 2020 (Dassault Systèmes SOLIDWORKS Corp., Waltham, MA, USA). The development of the devices followed the alignment of the flowchart in Figure 1.

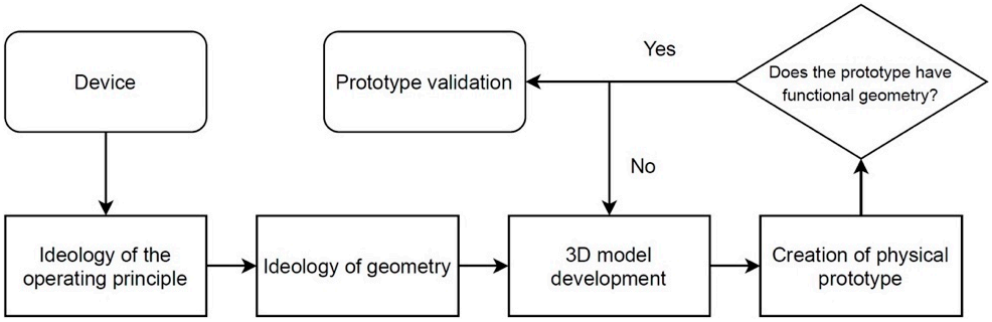

Figure 1. Flowchart of design development.

The first model resulted from a combination of the device designed by Gerace [8] and an opening and closing mechanism similar to a tensioner. The opening mechanism is composed of three threaded elements in which the user, when turning the central element, opens or closes the device, depending on the chosen direction, moving the side elements simultaneously. In this first version, the claws had a pivot system and were produced in a flexible material, thermoplastic polyurethane (TPU). Ergonomics was also considered,

especially in the region of contact between the thigh and the device, to make the experience of opening the thighs as pleasant as possible. This prototype also sought to guide the user to the correct use, demonstrating that its geometry is intuitive to manipulate. Figure 2 illustrates the results of the first idea, designed as a mechanical device.

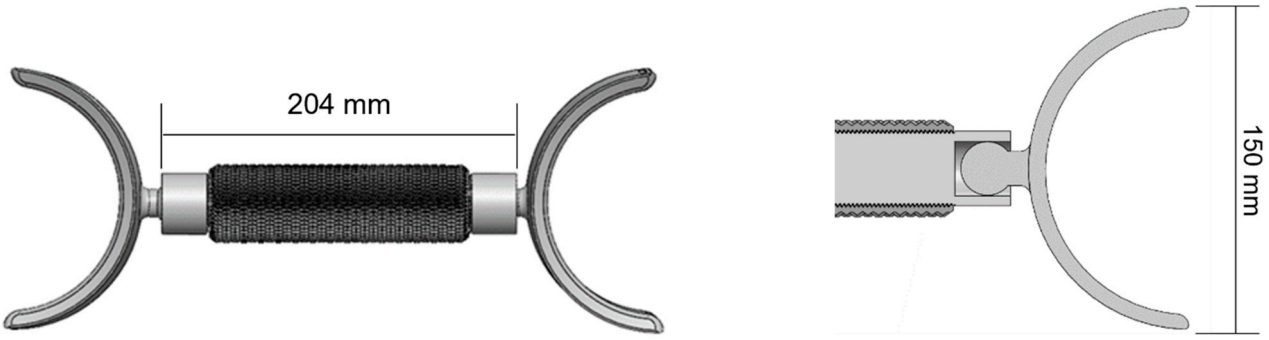

(**a**) (**b**)

Figure 2. 3D model of the mechanical device: (**a**) Global visualization; (**b**) Detail of pivot system.

As the literature does not give results concerning the quantification of the force made in the adduction movement in the sitting position, particularly for patients with spinal cord injury, the possibility of introducing the ability to quantify the force exerted on the system under development was studied. To this purpose, a load cell with reduced dimensions was selected, from the Interface brand, reference WMC-500, with a load capacity of 2.22 kN. The changes went through creating a "bed" where the load cell rests, and the material and system fix the device's claws. The new fixation system was subdivided, having a fixed claw with a tightening design between screw and nut and another claw, which fits in the load cell, with a pin-type system. The screw-nut fixation system had high rigidity. Therefore, one of the fixed side elements was changed so that a bearing was attached to give some freedom for adjusting the claw to the position. Consequently, the central part underwent modifications, increasing the thread on the side where the instrumented side element was presented and decreasing the thread on the fixed side element, reaching the instrumented device. Version 1 is represented in Figure 3.

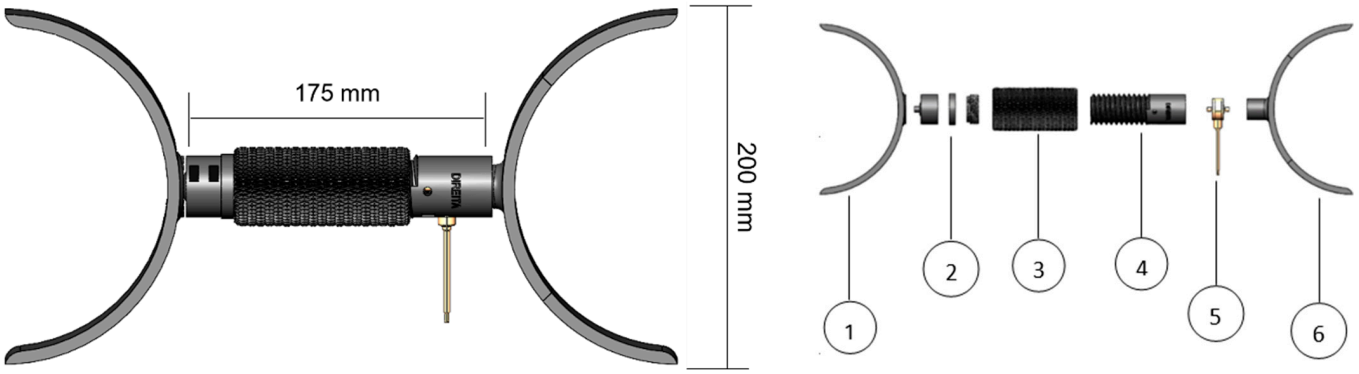

(**a**) (**b**)

Figure 3. 3D model of the instrumented device for force measurement: (**a**) Global visualization; (**b**) Detail with components, (1)—fixed claw, (2)—fixed side element, (3)—central element, (4)—mobile side element, (5)—load cell, (6)—instrumented claw.

The results obtained from the experimental tests, both in healthy volunteers and in patients present in Section 3.2, allow improving the mechanical device for a motorised

version. With the need to couple an embedded micro-motor, the geometries of some components changed, such as the clamping system of the claws, the mobile side element, and the central element. Figure 4 shows the 3D model of this version of the device. The diagram in Figure 4b represents the cable connections inside the central element where the end limit switches are coupled.

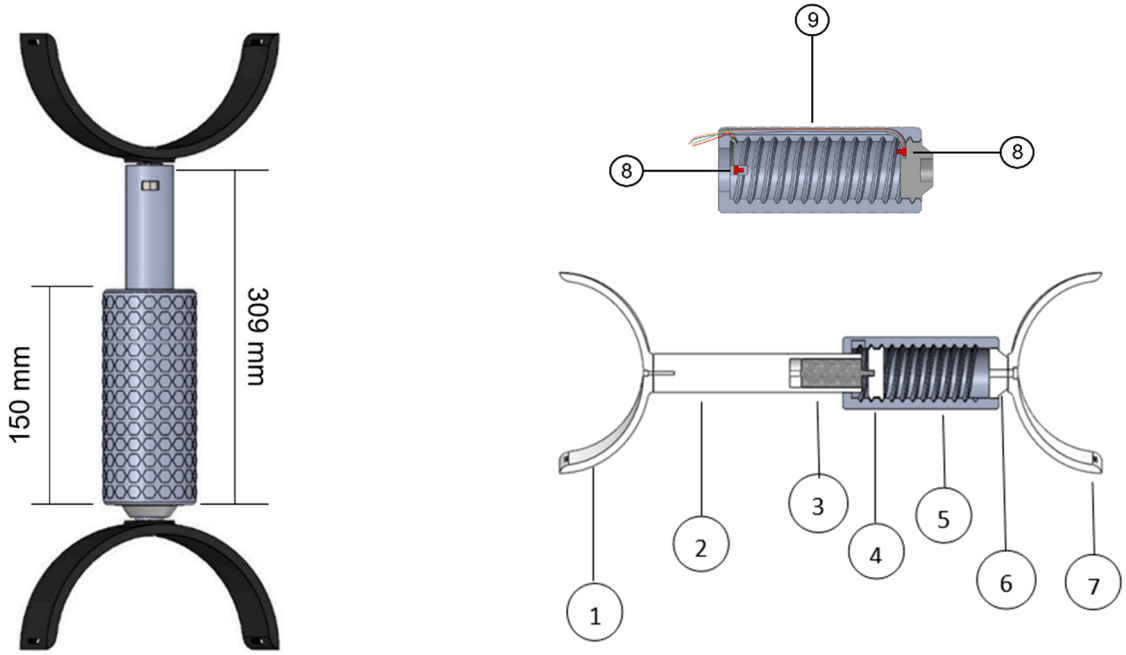

(**a**) (**b**)

Figure 4. 3D model of the motorised device: (**a**) Global visualization; (**b**) Detail with components, (1)—motor grip, (2)—movable side element, (3)—DC motor, (4)—threaded element, (5) central element, (6)—fastening element, (7)— fixed grip, (8)—positioning of end limit switches, (9)—embedded wire for signal transport.

The DC motor, the joystick, and the microcontroller to manage the device stroke, as well as safety limits, have been incorporated into a patient-accessible control box (Figure 5a). One of the aspects referred as a barrier in the self-catheterisation process is the difficulty in visualizing the insertion area. Therefore, a system was developed that allows anchoring a mirror (Figure 5c) or a camera (Figure 5b), an essential feature in this device.

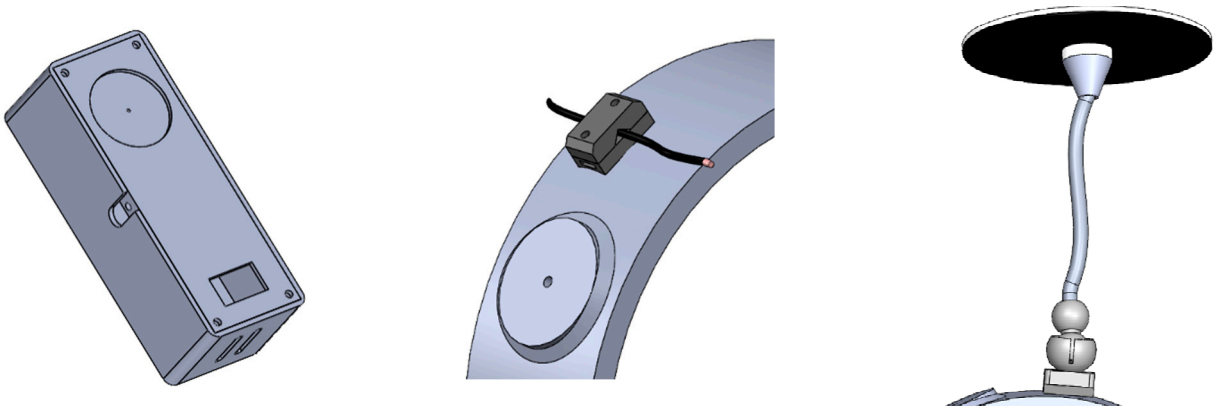

(**a**) (**b**) (**c**)

Figure 5. Add-ons: (**a**) Control unit; (**b**) Anchoring the camera; (**c**) Mirror anchor.

2.2. Production of Prototypes

The idea concerning the project's development was to use additive manufacturing to improve the costs of the mechanical components and implement "green" thinking with possible recycled materials. In the mechanical device, the material chosen for the claws was the polyethene glycol-ethylene terephthalate (PETG) due to its characteristics. The pivot system was produced in a flexible material, thermoplastic polyurethane (TPU). In the motorised model, the material of the mechanical components was changed to polylactic acid (PLA) due to its best characteristics associated with the friction and coupling of the motor. As a complement to the devices, pads were created in Elastosil M 4512 from the Wacker brand, offering greater comfort and easy cleaning. The anchoring systems for the mirror and the camera were produced with PETG. Table 1 shows the mechanical characteristics of the material used for additive manufacturing.

Table 1. Properties of the material used for additive manufacturing.

Material	Specific Mass ρ (kg/m^3)	Young's Modulus E (MPa)	Tensile Strength σc (MPa)	Poisson's Ratio ν
PETG	1420	2960	57.3	0.37
PLA	1240	3500	70.0	0.36
TPU	1120	26	45.0	0.39
Elastosil M4512 *	1190	-	3.5	-

* Hardness Shore A: 20.

As the different models were developed, produced prototypes allow testing various aspects of their functionality, such as ergonomics and design. Figure 6a shows an example of 3D prototyping, with a Prusa i3 mk3s+ equipment, producing the mechanical components in the respective materials mentioned above (example in Figure 6b).

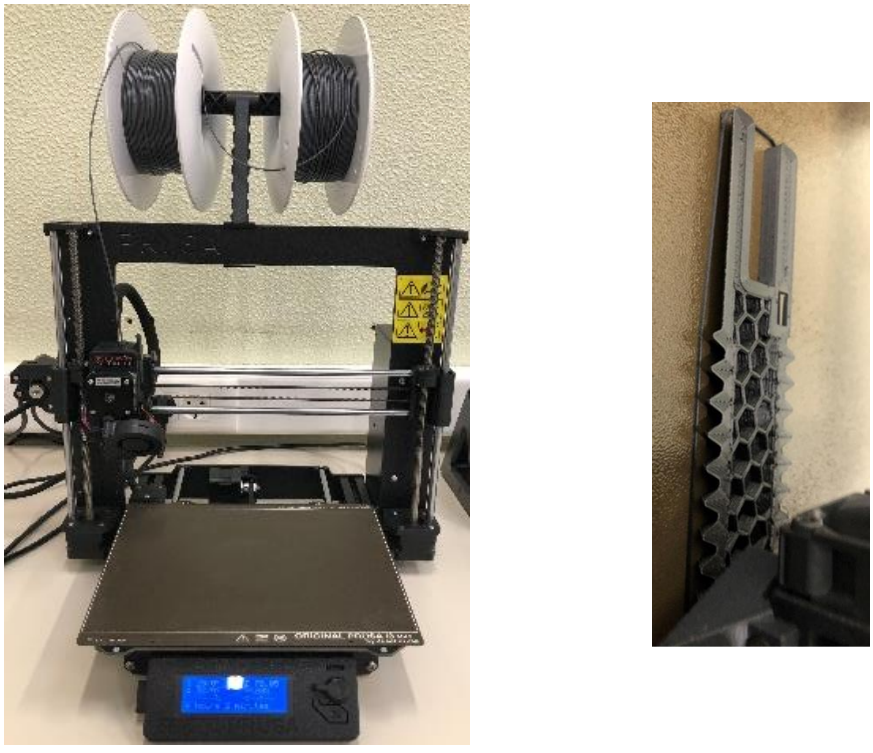

(**a**) (**b**)

Figure 6. (**a**) Prusa i3 mk3s+ equipment; (**b**) Example of a printing detail.

2.3. Real Devices

Figure 7 shows the final mechanical device obtained after production, showing the mirror system coupled to one side.

Figure 7. Mechanical device with the mirror system coupled.

The instrumented device is present in Figure 8a, with all the components assembled but without the mirror or the camera. A National Instruments data board (NI cDAQ-9174 Chassis and NI 9219 Acquisition Module) was used to connect the load cell by means of a developed LabView program running on a PC.

(**a**) (**b**)

Figure 8. (**a**) Instrumented device; (**b**) Interface of Labview program to connect the load cell.

Figure 8b shows the interface with the user for the load cell. The program allows watching, in real-time, the force applied by the user and was developed to provide an automatic calibration of the load cell, the register of the force/time, and the generation of a final report with the data acquired.

Four open positions of the system can be considered as predefined, as shown in Figure 9, which corresponds to the most closed (0 mm) and 20, 40 and 60 mm of opening.

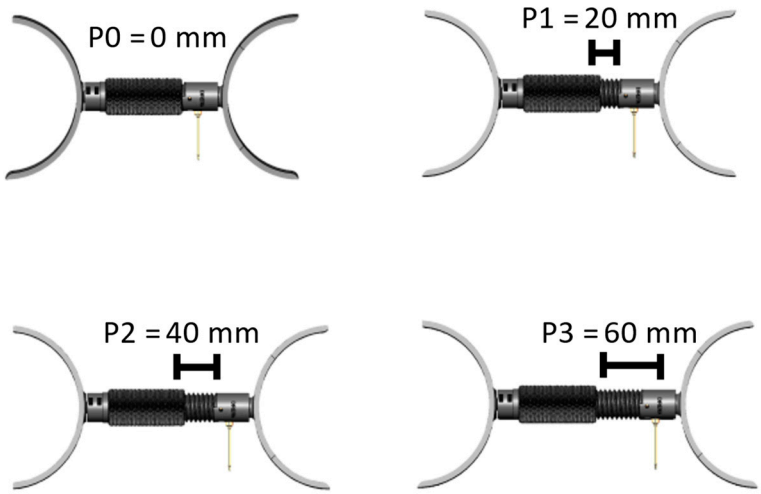

Figure 9. Device positions considered in the tests.

The motorised device is shown in Figure 10a. The connection of the control unit (Figure 10b) to the device is made through a cable mounted with a protection system, already referenced in Section 2.1, Figure 4b, called end limit switches, which turns off the motor as soon as it reaches the minimum or maximum allowed stroke.

(**a**) (**b**)

Figure 10. (**a**) Motorised device: (1) Camera with adjustable cable; (**b**) Detail of the command unit: (2) Button on/off; (3) Joystick.

2.4. Finite Element Models

Although the developed systems have been experimentally tested, the finite element method [24] was also implemented to analyse their structural behaviour. For this purpose, two models were created, considering the instrumented system and the motorised system, given some of its components' differences in geometry and cross-sections. The models were implemented using the Solidworks®software, with simplified geometry, to facilitate its definition by removing elements that would not influence the analysis. The study considers the worst position of the devices, with its extended opening.

The instrumented device is generally PET, while the motorised device is made of PLA. The materials are considered to have isotropic characteristics, an accepted simplification in numerical models. Thus, finite element models consider the mechanical characteristics described in Table 1.

The models assumed isotropic linear elastic properties for all the components. They were defined with tetrahedral parabolic solid elements (solid elements from Solidworks

library), with 3 degrees of freedom per node, representing the translations in the three orthogonal directions.

2.4.1. Instrumented Device

For the instrumented version of the device, the simplification of the geometry considers only the two central components, namely the nut and screw, as they are the most critical parts (Figure 11). The boundary conditions for the model consider the restriction of all degrees of freedom on the end face of the nut-type structural element (most rigid component). The force value and condition were based on the experimental results obtained from the tests with patients. The 235 N force was applied on the surface of the screw element (uniformly distributed and perpendicular to the surface), which translates the maximum force exerted by the volunteer's legs in the device for the considered position.

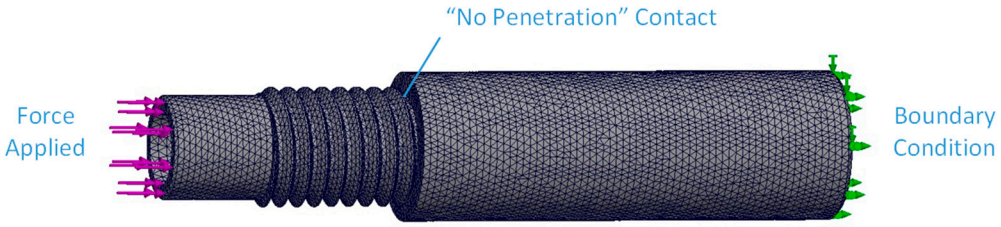

Figure 11. Visualization of the mesh, boundary conditions, and force applied in the finite element model of the instrumented device.

A study of convergence for the mesh was carried out, based on the energy of deformation, considering the maximum value of the resulting displacement in the model. Viewing the typology of the geometries under analysis and using the mesh-type option in the software, the maximum and minimum dimensions of the model were successively adjusted. The displacement stabilisation was obtained from elements between 0.5 mm and 2.5 mm. The contact between the surfaces considers the "no penetration" definition.

2.4.2. Motorised Device

For the motorised model, the geometry considers all the structural components. The opening length was kept the same as the instrumented device, corresponding to the worst position. The boundary and load conditions adopted also simulate the situation of a user exerting force on the device.

As this model considers the two claws, the option for boundary condition was to keep the nut component wholly anchored to the user's leg, with all degrees of freedom constrained in its contact surface. The other claw allows movement and is considered for load application. Two different force conditions were applied. The first one was based on the symmetry of the force, which simulates the situation of a user with the dimensions of the leg adapted to the size of the claw. The other considers some eccentricity, simulating the situation in which the dimensions of the limb are larger than those of the claw, as shown in Figure 12.

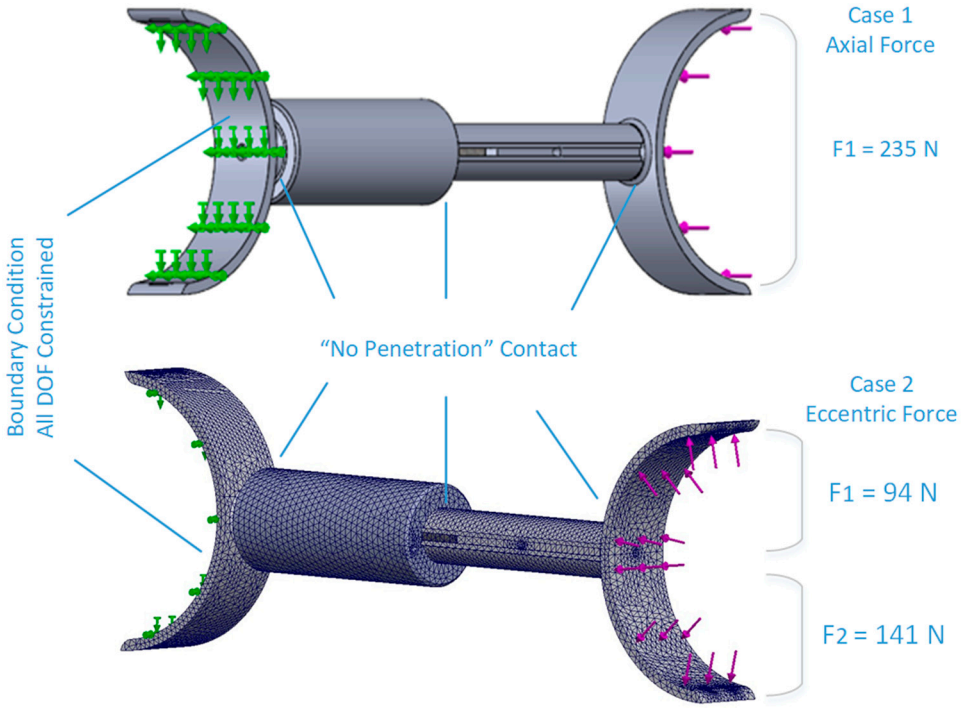

Figure 12. Load and boundary conditions for both situations.

The contact between the surfaces considers the "no penetration" definition. The mesh convergence of the model was performed following the same methodology as for the instrumented model, based on the comparative analysis of the maximum resulting displacements and their location, leading to elements that ranged from 0.98 mm to 5 mm.

2.5. Experimental Tests

As referred, the experimental tests were performed with the instrumented device, considering two groups of volunteers, namely healthy young students from the Coimbra School of Engineering and patients with spinal cord injury from the Hospital Rovisco Pais.

The experimental test protocol with volunteers was prepared following the Declaration of Helsinki. It was approved by the Ethics Committee of the Polytechnic of Coimbra (Reference no. 118_CEIPC2/2020) for the healthy volunteers and according to the hospital rules for the spinal cord injury volunteers. Each volunteer was assigned to a code with no identity records, safeguarding the necessary confidentiality.

Data statistical analysis was performed with two different statistical software: Microsoft Excel and IBM® SPSS® Statistics. With Excel, the data set acquired from each volunteer was studied to assess his/her behaviour throughout the experiment. The evolution of the peak strength of each volunteer was studied, and there could be a comparison of the various curves according to relevant parameters. With statistical analysis software IBM SPSS, the results obtained from the device for each volunteer were processed to verify the existence of correlations between the acquired data to validate the device and obtain valid biometric conclusions.

2.5.1. Tests with Healthy Young Volunteers

Concerning the experimental test, age was considered as an inclusion criterion. Firstly, the objectives and methodology of the study were presented to the volunteer, and they signed a form giving free and informed consent. After this, the protocol consisted of acquiring several biometric values, such as sex, age, height, weight, body mass index (BMI), body fat percentage, skeletal muscle percentage, visceral fat level, and resting kilocalories. Then, the volunteer answered a questionnaire with additional data on the history of injuries

and the quantity and quality of their weekly physical activity. The existence of pathologies in the lower limbs for less than five years was considered an exclusion criterion.

After completing the questionnaire, the volunteer sat in a comfortable position, as shown in Figure 13.

Figure 13. Position of the volunteer to perform the test of the instrumented device.

When the volunteer was ready, four positions in an opening interval of (0, 60) mm were considered for the acquisition: P0 force values, corresponding to the initial force positions (opening of 0 mm); P1 force (position of 20 mm); P2 force (open position of 40 mm); P3 force (open position of 60 mm). All these positions are represented in Figure 9. The volunteer was asked to contract their legs against the device as hard as possible in each position. The volunteer rested for 1 minute between sections while adjusting the device to the next position. During testing, the volunteer could monitor the strength in real-time in the GUI shown, previously, in Figure 8.

2.5.2. Tests with Volunteers with Spinal Cord Injury

The setup of tests with patients with spinal cord injury was referred to in the previous section and is represented in Figure 14. In this case, the test procedure differed in some aspects. Due to the particular health situation of the volunteers, there was no filling out of the device evaluation questionnaire or the graphic interface. Additionally, the only data acquired were age, height, weight, sex, and opening in the *Budda position*, as they were considered enough to understand and compare the device's performance. In particular, the aim of acquiring the opening in the *Budda position* was to normalize the device size relating it to the volunteer's height. Clinical data such as the gradient of muscle function, grade AIS (Abbreviated Injury Scale) and type and location of paralysis were also needed to understand whether the volunteer's grade of disease would influence strength.

Figure 14. Setup of tests at Hospital Rovisco Pais.

The specific position of the volunteer was maintained, additionally, the wheelchair usually used by the user was considered. This type of testing is closer to real use by this type of patient.

3. Results

3.1. Numerical Results

3.1.1. Instrumented Device

The von Mises stress distribution obtained is shown in Figure 15, presenting a uniform distribution and values lower than the material yield stress. As can be observed, the contact regions show a peak of 33.2 MPa, corresponding to the beginning of the contact for the threaded element, associated with the geometric conditions of the model. Based on the results and for the requirements of the model, an adequate strength can be considered.

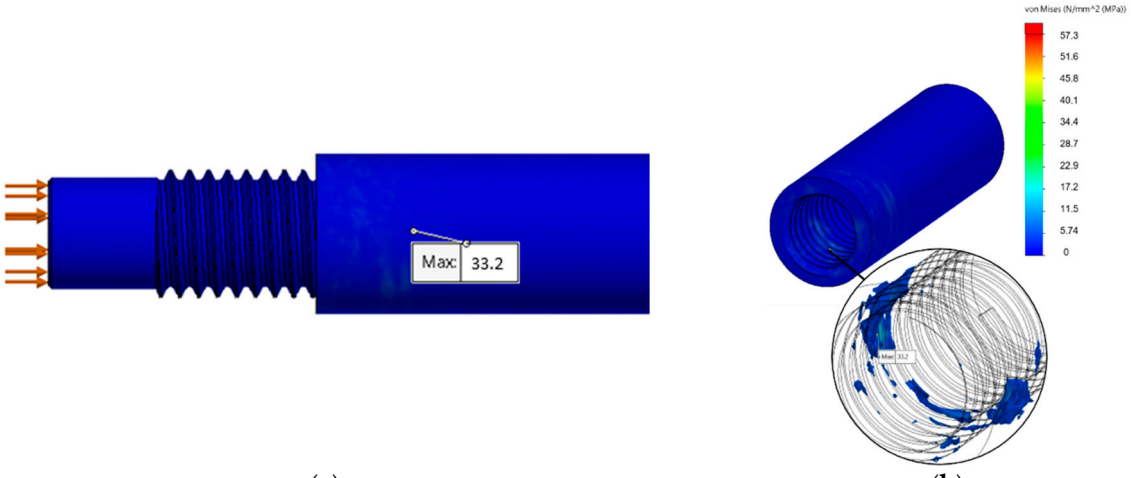

(**a**) (**b**)

Figure 15. Distribution of von Mises stress for the instrumented device: (**a**) View of the global model; (**b**) Detail of von Mises stress distribution in the contact region.

3.1.2. Motorised Device

In the case of the motorised model, for both load cases, all the components presented von Mises stress values lower than the yield stress of considered PLA, due to its characteristics, particularly with friction between the central element and the threaded element.

Table 2 summarises the more significant value of von Mises stress on each part for both force conditions. The obtained results show an adequate strength for the model.

Table 2. Maximum values of von Mises stress on the components.

Component	Maximum von Mises Stress (MPa)	
	LOAD CASE 1	LOAD CASE 2
Motor grip	13.15	18.39
Movable side element	5.84	7.67
Central element	12.55	10.04
Threaded element	19.10	104.30
Fastening element	0.73	4.89
Fixed Grip	0.51	4.17

Figure 16 shows the contact zone between the elements for load case 1, where a stress peak can be observed at the beginning of the contact for the threaded element (19.1 MPa). It must be noted that the positioning of the screw is the most unfavourable. Moreover, geometric conditions associated with the end of the threat and the mesh performed contributed to the peak in the initial contact zone. These results show consistency that the value is minimal in relation to the material's yield strength.

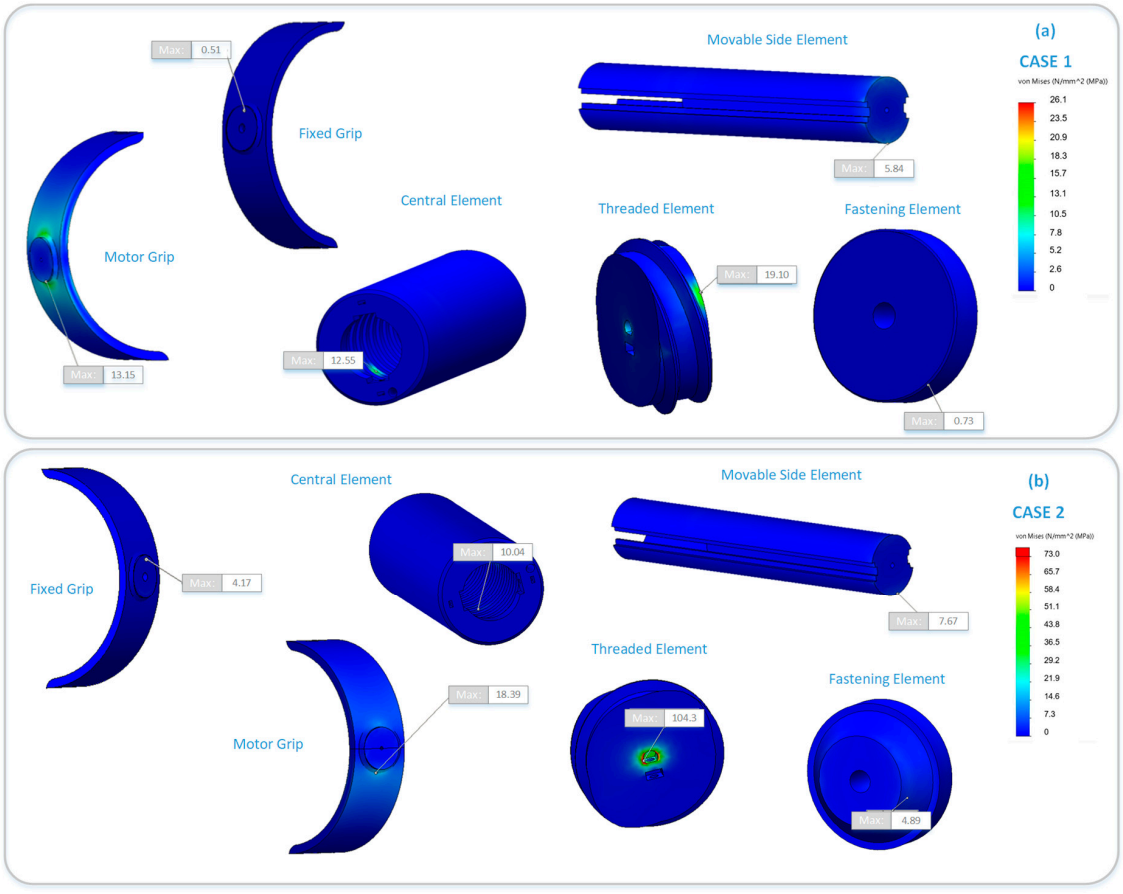

Figure 16. Distribution of von Mises stress in the mechanical components: (**a**) Load Case 1—axial force; (**b**) Load Case 2—eccentric force.

In the case of load case 2, as the force was eccentric, the more significant values of the von Mises stress were present in the contact zone between the motor shaft and the cavity where it was coupled. This peak was due to the bending phenomenon, as shown in Figure 17, representing the model's distribution of the resultant displacement. A maximum value of 7.91 mm (load case 1) and 14.44 mm (load case 2) was obtained for the resultant displacements.

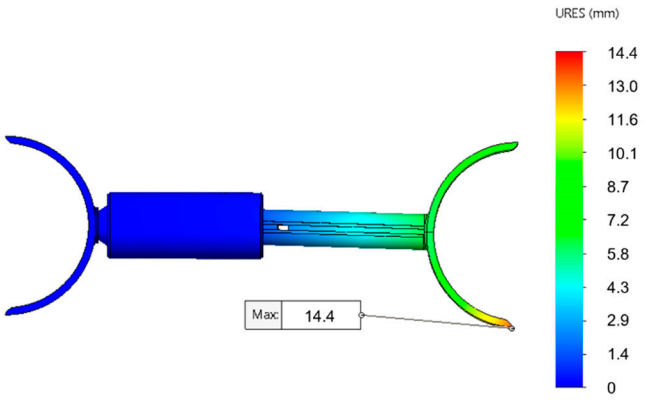

Figure 17. Distribution of resultant displacements for load case 2.

3.2. Experimental Results

3.2.1. Tests with Healthy Volunteers

A total of 32 volunteers were included in the study, with an equal number of female and male individuals coming from the student community of ISEC. Table 3 shows the characterisation of the sample of volunteers.

Table 3. Characterisation of the volunteers from ISEC.

	Mean	Maximum	Minimum
Age	22	27	19
Height (cm)	169.95	186.00	155.00
Weight (kg)	75.51	121.80	47.50
BMI	26.16	50.70	18.80
% Body Fat	32.82	59.90	16.20
% Skeletal Muscles	30.44	43.00	15.90

The volunteer's opinion concerning the system's usability was obtained from a questioner with statements that could be classified between 1 (strongly disagree) and 5 (strongly agree). The device obtained a rating of 4.55 out of 5 values for the ergonomic parameters. The graphical interface with its layout, understanding, and visual appearance scored 4.56. The final position and the claws obtained the lower rating (4.09) in terms of comfort. Regarding the difficulty level, the volunteers considered both the handling and the execution of the movement easy to perform (4.56).

The measures of central tendency (mean—M) and dispersion (standard deviation—SD) were determined using descriptive statistics to characterise the sample. Table 4 shows the average strength, which generally varies in the interval (179.04, 212.76) having the extreme forces in the final and initial position, respectively, and a standard deviation in (71.80, 88.60).

Table 4. Means (M), standard deviations (SD), minimums, and maximums for the total sample forces of the volunteers from ISEC.

	Total Sample (n = 32)				
	M	**SD**	**Median**	**Minimum**	**Maximum**
Force P0	212.76	88.60	224	70.33	416.92
Force P1	206.28	78.12	197	75.77	345.22
Force P2	188.52	71.80	207	65.40	371.81
Force P3	179.04	80.02	207	46.10	327.27

The comparison between gender is present in Table 5, with the measures of central tendency for independent samples.

Table 5. Means (M), standard deviations (SD), minimums, and maximums for the independent samples by gender.

	Male (n = 16)				Female (n = 16)			
	M	**SD**	**Minimum**	**Maximum**	**M**	**SD**	**Minimum**	**Maximum**
Force P0	257.32	88.09	70.33	416.92	198.81	72.64	96.35	295.70
Force P1	244.14	71.34	10.22	345.22	191.70	71.10	87.32	283.84
Force P2	225.22	57.04	68.00	371.81	159.92	68.04	65.40	251.24
Force P3	212.76	68.39	51.48	327.27	150.50	77.78	60.13	264.66

To complement the results expressed in Table 5, the box plot of Figure 18 shows the influence of gender on the strength value in each position.

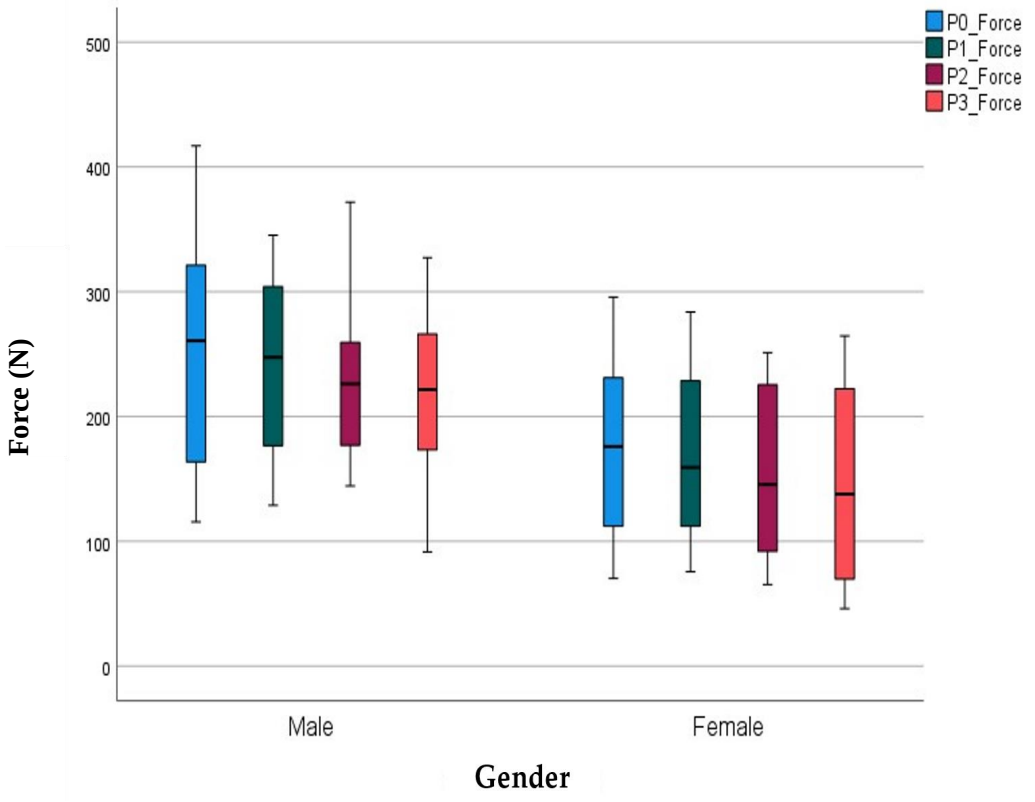

Figure 18. Boxplot of forces by gender.

To corroborate the previous statement, *t*-tests were performed with a significance of 5% (and 95% confidence intervals) for the equality of the means of the forces, obtaining the results described in Table 6.

Table 6. *t*-test for equal force averages in the healthy population (independent samples test).

Force	Equal Variances	Levene's Test Equality of Variances		*t*-Test for Equality of Means						
				t	df	*p*-Value	Mean Difference	Std. Error Difference	95% Confidence Interval of the Difference	
		F	Sig.						Lower	Upper
P0	Assumed	0.691	0.413	2.71	30.00	0.011	77.30	28.55	18.99	135.59
	Not Assumed			2.71	28.95	0.011	77.30	28.55	18.99	135.59
P1	Assumed	0.054	0.818	2.70	30.00	0.011	68.02	25.18	16.60	119.44
	Not Assumed			2.70	30.00	0.011	68.02	25.18	16.60	119.44
P2	Assumed	2.333	0.137	3.25	30.00	0.003	72.05	22.20	26.72	117.39
	Not Assumed			3.25	29.11	0.003	72.05	22.20	26.72	117.39
P3	Assumed	1.121	0.298	2.65	30.00	0.013	68.56	25.89	15.68	121.44
	Not Assumed			2.65	29.52	0.013	68.56	25.89	15.68	121.44

To analyse the influence of biometric parameters, Pearson correlations were determined. There were several correlations between weight and BMI ($\rho = 0.883$) and the percentage of skeletal muscles and body fat ($\rho = -0.908$). Another moderate linear correlation of $0.39 < \rho < 0.477$ was observed between the rate of skeletal muscles and the various forces. Some graphs, represented in Figure 19, were constructed to understand the force behaviour with the variation of the related biometric data.

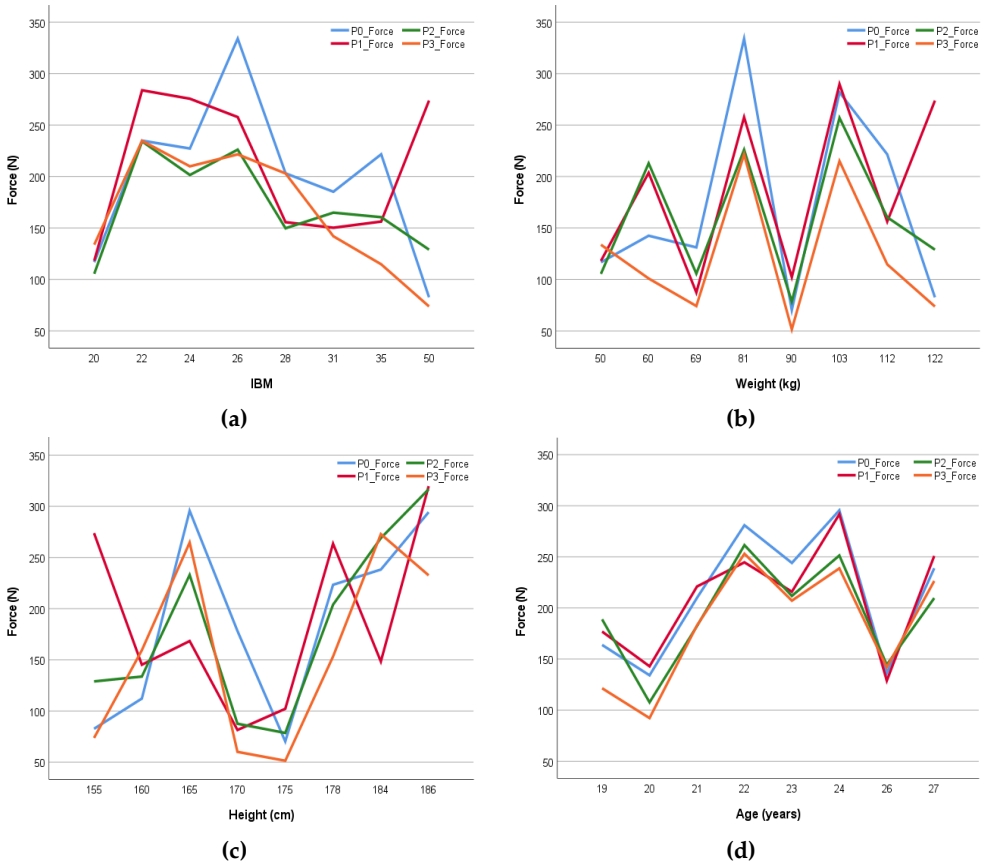

Figure 19. Graphical visualisation of force against some biometric data: (**a**) Force—IMC; (**b**) Force—Weight; (**c**) Force—Hight; (**d**) Force—Age.

The correlations between the forces were analysed using the Pearson correlations shown in Table 7.

Table 7. Pearson's correlations for ISEC volunteer strengths.

	Force P0	**Force P1**	**Force P2**	**Force P3**
Force P0	1	0.671	0.716	0.732
Force P1	0.671	1	0.784	0.626
Force P2	0.716	0.784	1	0.814
Force P3	0.732	0.626	0.814	1

3.2.2. Tests with Patients

The sample used in the present tests consists of ten volunteers (five female and five males) with spinal cord injury (SCI) from the Hospital Rovisco Pais. The volunteers, aged between 30 and 72 years (M = 62.6; SD = 13.074), had heights between 145 cm and 183 cm (M = 167.7; SD = 11.71) and weights between 46 kg and 84 kg (M = 70.6; SD = 10.56). Regarding their clinical data, 50% (n = 5) had a gradient of muscle function of 4, 10% (n = 1) of 3, 30% (n = 3) of 2, and 10% (n = 1) of 0.

The AIS scale describes the functional behaviour of the persons with spinal cord injury. It is divided into 5 degrees: A (complete), B (sensory incomplete), C (motor incomplete), D (motor incomplete), E (normal). As far as the AIS degree was concerned, the one with the highest percentage of volunteers, 80% (n = 8), was D, with the remainder being degree C (n = 1, 10%) and degree A (n = 1, 10%).

The measures of central tendency (mean—M) and dispersion (standard deviation—SD) for the total sample were calculated using descriptive statistics and are shown in Table 8.

Table 8. Means (M), standard deviations (SD), minimums, and maximums for the total sample forces for the patients.

	Total Sample (n = 10)				
	M	**SD**	**Median**	**Minimum**	**Maximum**
Force P0	106.29	78.40	87	19.76	235.47
Force P1	118.95	69.46	89	33.12	233.07
Force P2	123.10	65.28	121	44.17	214.44
Force P3	130.32	76.33	109	33.29	235.47

Similar to what was discussed in Section 3.2.1 and to investigate gender differences, independent samples were characterised, and the results can be seen in Table 9.

Table 9. Means (M), standard deviations (SD), minimums, and maximums for the independent sample.

	Male (n = 5)				**Female (n = 5)**			
	M	**SD**	**Minimum**	**Maximum**	**M**	**SD**	**Minimum**	**Maximum**
Force P0	163.01	66.00	60.60	235.47	49.56	37.79	19.76	112.51
Force P1	173.34	52.03	89.58	233.07	64.55	27.40	33.12	87.41
Force P2	175.58	36.79	118.10	214.44	70.62	36.76	44.17	123.52
Force P3	194.78	44.63	122.16	235.47	65.86	27.01	33.29	96.20

The t-tests were performed with a significance of 5% (and 95% confidence intervals) for the equality of the means of the forces, obtaining the results described in Table 10.

Table 10. *t*-test for equal force averages for tests at Hospital Rovisco Pais (independent samples test).

Force	Equal Variances	Levene's Test Equality of Variances		*t*-Test for Equality of Means						
				T	df	*p*-Value	Mean Difference	Std. Error Difference	95% Confidence Interval of the Difference	
		F	Sig.						Lower	Upper
P0	Assumed	0.718	0.422	3.34	8.00	0.010	113.45	34.01	35.02	191.88
	Not Assumed			3.34	6.37	0.014	113.45	34.01	31.38	195.52
P1	Assumed	0.342	0.575	4.14	8.00	0.003	108.80	26.30	48.15	169.44
	Not Assumed			4.14	6.06	0.006	108.80	26.30	44.60	172.99
P2	Assumed	0.164	0.696	4.51	8.00	0.002	104.96	23.26	51.33	158.59
	Not Assumed			4.51	8.00	0.002	104.96	23.26	51.33	158.59
P3	Assumed	0.666	0.438	5.53	8.00	0.001	128.91	23.33	75.12	182.71
	Not Assumed			5.53	6.58	0.001	128.91	23.33	73.03	184.79

Table 11 shows the Pearson's correlations concerning the forces obtained from the tests in Rovisco Pais Hospital.

Table 11. Pearson's correlations of the test's strength at Rovisco Pais.

	Force P0	Force P1	Force P2	Force P3
Force P0	1	0.900	0.757	0.789
Force P1	0.900	1	0.942	0.948
Force P2	0.757	0.942	1	0.975
Force P3	0.789	0.948	0.975	1

4. Discussion

In the literature, several studies aim to quantify the strength in the lower limbs. Most focus on the abductor muscle and the hip abduction movement. In addition, the sample is usually made up of high-competition athletes or people who have undergone surgery, such as arthroplasty. The present study differs, as it focuses on the adduction movement to the "sitting" position in a healthy population with no history of pathologies in the lower limbs and people with spinal cord injury. Another objective of the studies was to acquire data and information that would help design a safe and applicable device to support the self-catheterisation process.

In addition to validating the device and evaluating its applicability, the tests were performed to provide a basis for strength reference values for future work. With the results obtained in both tests, it can be concluded that, in general, females have lower strength values than males. Force values, in the case of healthy volunteers, are in the range (46, 417) N while the values of the Rovisco Pais tests of persons with a SCI are in the range (20, 235) N. Through Pearson correlations and designed graphics, it was possible to corroborate the robustness of the device demonstrated by the numerical analysis.

Through the research and all the feedback acquired during hospital tests, it was possible to design a device that supports the process, not only in the person's position but also in the visualisation of the probe insertion area with the mirror (an add-on that already exists in other devices) or camera (an innovative add-on from the current devices). Another advantage is the possibility of being a 2 in 1 device. The instrumented version makes it possible to couple the add-ons and is a measurement and support device. Another difference is motorisation. Currently, there are no devices in this area that allow commanded opening. The survey results show that dimensions, contact surface, aesthetics, and ergonomics adopted are suitable for using the devices.

The values acquired will serve as a reference for future work.

5. Conclusions

The present work involved developing and studying a biomechanical device to support the self-catheterisation of spastic patients. The work involved the construction of several models of the components that make up the device, reaching the final geometry after verifying the existence of a link between geometry, functionality, ease, simplicity of use, and the prediction of its structural behaviour. This link was achieved at three relevant levels: clinical adherence, with emphasis on the ease of performing the self-catheterisation technique; mechanical behaviour, carried out numerically through finite element models and with experimental tests carried out on volunteers; the production facility by additive manufacturing, with a design that simplifies the printing process. Several experimental trials have been implemented in healthy volunteers and individuals with spinal cord injury.

The data collected was analysed, and the results obtained allowed us to draw conclusions that compared the two groups on various factors. In the case of healthy volunteers, the results allowed the creation of a reference pattern that will be useful in future work in the context of this type of patient. The ratings attributed to the device's functionality showed that it fits the objectives defined for the work while also being easy to use. It is essential to mention the mechanical resistance demonstrated in the final version of the device, even with the production of components by additive manufacturing.

The observation of the tests showed that the device developed can support the self-catheterisation process. Despite the main objective of self-catheterisation, the system's design made it possible to quantify the strength of the adductors for the sitting position during the execution of the adduction movement, particularly relevant for spastic patients. It can be adapted to assist in the rehabilitation of patients with pathologies in which the type of movement and force exerted can be recommended. This solution will also help improve individuals' self-esteem and independence with spinal cord injury, providing the confidence necessary to adhere to the process.

Author Contributions: Conceptualization, M.C., L.R., N.C., J.L. and F.C.; methodology, M.C., L.R., J.L. and F.C.; software, V.M.; validation, D.R., F.C. and J.L.; writing—original draft preparation, M.C. and L.R.; writing—review and editing, J.L., F.C., D.R. and F.M. All authors have read and agreed to the published version of the manuscript.

Funding: This research received no external funding.

Institutional Review Board Statement: The experimental tests were conducted according to the guidelines of the Declaration of Helsinki and approved by the Ethics Committee of the Polytechnic of Coimbra (Reference no. 118_CEIPC2/2020) and the rules of the Hospital Rovisco Pais.

Informed Consent Statement: Informed consent was obtained from all subjects involved in the study.

Data Availability Statement: Not applicable.

Acknowledgments: This research was sponsored by FEDER funds through the COMPETE—Programa Operacional Factores de Competitividade program and by national funds through the Fundação para a Ciência e a Tecnologia (FCT) under project UIDB/00285/2020.

Conflicts of Interest: The authors declare no conflict of interest.

References

1. Assis, G.M.; Faro, A.C.M. Clean intermittent self catheterization in spinal cord injury. *Rev. da Esc. de Enferm. da USP* **2011**, *45*, 282–286. [CrossRef]
2. Shenot, P.J. Bexiga neurogénica. Available online: https://www.msdmanuals.com/pt/profissional/dist%C3%BArbios-geniturin%C3%A1rios/dist%C3%BArbios-miccionais/bexiga-neurog%C3%AAnica (accessed on 14 October 2020).
3. Mazzo, A.; Souza-Junior, V.D.; Jorge, B.M.; Nassif, A.; Biaziolo, C.F.; Cassini, M.F.; Santos, R.C.R.; Mendes, I.A.C. Intermittent urethral catheterization—Descriptive study at a Brazilian service. *Appl. Nurs. Res.* **2014**, *27*, 170–174. [CrossRef] [PubMed]
4. Panicker, J.; Seth, J.; Haslam, C. Ensuring patient adherence to clean intermittent self-catheterization. *Patient Prefer. Adher.* **2014**, *8*, 191–198. [CrossRef] [PubMed]
5. Baczkoski, J.S. Mirror assembly for patients with personal hygiene problems. U.S. Patent 4,257,680, 24 March 1981.
6. Levy, E.A. Mirror assembly to be held between the knees of a user. U.S. Patent 3,411,842, 19 November 1968.

7. Billau, B.W.; Howland, D.R. Self-catheterization for the woman with quadriplegia. *Am. J. Occup. Ther.* **1991**, *45*, 366–369. Available online: https://ajot.aota.org/article.aspx?articleid=1875875 (accessed on 7 October 2020). [CrossRef]
8. Gerace, J.A. Mirror adapted for use in self-catheterizing procedures. U.S. Patent 5,311,366, 10 May 1994.
9. Alvi, H.I.; Cozzie, N.L.; Wilkinson, M.R.; Ochoa, A.; Eaton, B. Self-inspection apparatus. U.S. Patent 8602574, 10 December 2013.
10. Winther, S.B.; Foss, O.A.; Husby, O.S.; Wik, T.S.; Klaksvik, J.; Husby, V.S. A randomized controlled trial on maximal strength training in 60 patients undergoing total hip arthroplasty. *Acta Orthop.* **2018**, *89*, 295–301. [CrossRef]
11. Trudelle-Jackson, E.; Smith, S.S. Effects of a late-phase exercise program after total hip arthroplasty: A randomized controlled trial. *Arch. Phys. Med. Rehabilit.* **2004**, *85*, 1056–1062. [CrossRef]
12. Pinto, J.L.D. Dados Normativos e Normalizados de Força de Adução e Abdução da Anca em Jogadores de Futebol de Elite em Portugal. Ph.D. Thesis, Universidade Privada da Maia, Maia, Portugal, December 2020.
13. Unlu, E.; Eksioglu, E.; Aydog, E.; Aydoð, S.T.; Atay, G. The effect of exercise on hip muscle strength, gait speed and cadence in patients with total hip arthroplasty: A randomized controlled study. *Clin. Rehabilit.* **2007**, *21*, 706–711. [CrossRef] [PubMed]
14. Monaghan, B.; Cunningham, P.; Harrington, P.; Hing, W.; Blake, C.; Dohertya, D.O.; Cusack, T. Randomised controlled trial to evaluate a physiotherapy-led functional exercise programme after total hip replacement. *Physiotherapy* **2016**, *103*, 283–288. [CrossRef] [PubMed]
15. Muscle Controller by Kinvent. Hand-Held Dynamometer for Physios and Sport Pros. Available online: https://k-invent.com/k-forcemuscle-controller/ (accessed on 4 January 2022).
16. ForceFrame: Strength Testing System. VALD Performance. Available online: https://valdperformance.com/forceframe/ (accessed on 4 January 2022).
17. Cabrera, M.N.B.; Norris, J.A. Aparatus and method for evaluating hypertonic condition. U.S. Patent 2007/0027631A1, 1 February 2007.
18. Wang, T.Y.; Wu, C.Y.; Sutton, O.M. Spasticity quantification device. U.S. Patent 2016/0317066A1, 3 November 2016.
19. Husby, V.S.; Helgerud, J.; Bjørgen, S.; Husby, O.S.; Benum, P.; Hoff, J. Early maximal strength training is an efficient treatment for patients operated with total hip arthroplasty. *Arch. Phys. Med. Rehabilit.* **2009**, *90*, 1658–1667. [CrossRef] [PubMed]
20. Ström, H.; Huss, K.; Larsson, S. Unrestricted weight bearing and intensive physiotherapy after uncemented total hip arthroplasty. *Scand. J. Surg.* **2006**, *95*, 55–60. [CrossRef] [PubMed]
21. Gafner, S.; Bastiaenen, C.H.G.; Terrier, P.; Punt, I.; Ferrari, S.; Gold, G.; De Bie, R.; Allet, L. Evaluation of hip abductor and adductor strength in the elderly: A reliability study. *Eur. Rev. Aging Phys. Act.* **2017**, *14*, 5. [CrossRef] [PubMed]
22. Ryan, S.; Kempton, T.; Pacecca, E.; Coutts, A.J. Measurement properties of an adductor strength-assessment system in professional australian footballers. *Int. J. Sports Physiol. Perform.* **2019**, *14*, 256–259. [CrossRef] [PubMed]
23. Vega, E.C.; Jerez-Mayorga, D.; Payer, R.M.; Jara, C.C.; Guzman-Guzman, I.; Ponce, A.R.; Chirosa, L.J. Validity and reliability of evaluating hip abductor strength using different normalization methods in a functional electromechanical device. *PLoS ONE* **2018**, *13*, e0202248. [CrossRef]
24. Neto, M.A.; Amaro, A.; Roseiro, L.; Cirne, J.; Leal, R. *Engineering Computation of Structures: The Finite Element Method*; Springer: Berlin, Germany, 2015; ISBN 978-3-319-17709-0.